

QMC and the nature of dense matter: written in the stars?

J. D. Carroll

*Centre for the Subatomic Structure of Matter (CSSM), Department of Physics, University of
Adelaide, SA 5005, Australia*

Abstract. We discuss the recent progress in calculating the properties of ‘*hybrid stars*’ (stellar objects similar to neutron stars, classified by the incorporation of non-nucleonic degrees of freedom, including but not limited to hyperons and/or a quark-matter core) using the octet-baryon Quark-Meson Coupling (QMC) model. The version of QMC used is a recent improvement which includes the in-medium modification of the quark-quark hyperfine interaction.

Keywords: QMC, EOS, dense matter, neutron stars, hybrid stars, MIT, NJL

PACS: 26.60.Kp, 21.65.Qr, 12.39.-x

1. INTRODUCTION

The study of the QCD phase diagram is of great interest to the scientific community. Lattice QCD produces simulations which provide an insight into the $\{T > 0, \mu \simeq 0\}$ region of the phase diagram, whilst properties of QCD at finite chemical potential can be calculated using various models for dense hadronic matter (at $T \geq 0, \mu \gg 0$). In order to qualify the success of these models we require a method to test the predictions via experiment and observation. For finite chemical potentials, this requires tests at various relevant density scales. For low-density predictions we can compare calculations to experiments involving finite nuclei, but no experiment (to date) can probe the entire range of extreme densities believed to exist within neutron stars¹. We therefore turn our attention to proxy measurements which may support or refute our predictions, such as the masses and radii of pulsars.

We focus our attention on a particular model—the Quark-Meson Coupling model (QMC), which we shall describe in Section 2—that has seen much success at each of these density scales, and focus in particular on the high-density Equation of State (EoS) for infinite matter (see Section 3). In order to examine the effects of quark degrees of freedom at extremely high densities we model a phase transition between this hadronic EoS and a quark-matter EoS as described by several models (see Section 4). We examine the predictions for neutron star properties that arise from calculations involving the QMC EoS and the effect that the phase transition has on these properties in Section 5.

¹ In Ref. [1] the authors note that heavy-ion collisions may be able to provide insight into the properties of matter up the density range of $2-3\rho_0$.

2. QMC

The Quark-Meson Coupling (QMC) model [2] describes baryons as ‘bags’ of three confined quarks for which the energy-density is greater than that of the surrounding non-perturbative vacuum by $B \sim (180 \text{ MeV})^4$. These quarks are immersed in a mean-field of mesons which contribute to attractive scalar and repulsive vector potentials, which describe interactions in a similar way to Quantum Hadrodynamics (QHD). This model has seen much success in predicting the properties of finite nuclei, in particular hypernuclei (containing strange quarks) with the recent addition of a Λ - Σ hyperfine splitting contribution [2].

We model baryons influenced by scalar-isoscalar σ , vector-isoscalar ω , and vector-isovector ρ mesons, noting that the mean-field pseudoscalar-isovector π field contribution is zero due to parity considerations. We additionally include leptons ($\ell \in \{e^-, \mu^-\}$) interacting with baryons in beta-equilibrium in our calculations.

In QMC, the effective mass for the baryons has a quadratic form—incorporating the scalar polarizability d which self-consistently allows feedback of the scalar field—given by

$$M_B^* = M_B + \Sigma_B^s = M_B - w_B^s g_{\sigma N} \langle \sigma \rangle + \frac{d}{2} \tilde{w}_B^s (g_{\sigma N} \langle \sigma \rangle)^2, \quad (1)$$

where the factors w_B^s and \tilde{w}_B^s (the origins and values of which are discussed in further detail in Ref. [2]) account for the SU(6)-style coupling ratios for the various octet baryons $B \in \{N^{+,0}, \Lambda, \Sigma^{\pm,0}, \Xi^{-,0}\}$. The inclusion of hyperons into these calculations does not result in negative effective baryon masses—the occurrence of which is a shortcoming of QHD attributed to the linear effective mass, and the reason that we do not model hyperons in QHD—since the scalar potential responds to the strength of the scalar field in a way that prevents this. Indeed, the effective masses of all the baryons remain positive for any value of $\langle \sigma \rangle$ in QMC.

The couplings of the nucleons to the mesons in QMC ($g_{N\sigma}, g_{N\omega}, g_\rho$) are fitted such that the saturation properties of nuclear matter are reproduced in isospin symmetric nuclear matter. The nucleon-meson couplings and quantities that we reproduce are given in Table 1. The couplings of the hyperons to the isoscalar mesons are related to these nucleon-meson couplings via SU(6) spin-flavor relations, and while the couplings of the hyperons to the isovector meson are unified into a single value, each vertex term includes an isospin factor I_{zB} which splits the vector potentials within an isospin group.

TABLE 1. Meson-nucleon couplings and reproduced saturation properties of nuclear matter: energy per baryon; baryon density; and symmetry energy at saturation. The couplings are fitted to best reproduce the experimental values.

$g_{\sigma N}$	$g_{\omega N}$	g_ρ	$(\mathcal{E}/\rho_0 - \sum_B \rho_B M_B)$	ρ_0	a_4
8.278	8.417	8.333	-15.86 MeV	0.16 fm ⁻³	32.5 MeV

The hyperon Fermi momenta (and hence, densities) are determined via relations between the baryon chemical potentials, according to

$$\mu_i = B_i \mu_n - Q_i \mu_e = \sqrt{k_{F_i}^2 + (M_i + \Sigma_i^s)^2} + \Sigma_i^0, \quad (2)$$

where $B_i = +1 \forall i \in B$ and Q_i are respectively the baryon and electric charges (the latter in units of the proton charge) associated with the neutron and electron independent chemical potentials μ_n and μ_e ; and $\Sigma_i^{s,0}$ are the scalar and temporal components of the baryon self-energy.

In QHD, the baryon self-energies at Hartree level are calculated by considering the tadpole diagrams as modifications to the baryon propagator. Following the derivation of Ref. [3], the scalar component of the baryon self-energy is given by

$$\Sigma_B^s \text{ QHD} = -g_{\sigma B} \langle \sigma \rangle = -g_{\sigma B} \sum_{B'} \frac{g_{\sigma B'}}{m_\sigma^2} \frac{(2J_{B'} + 1)}{(2\pi^3)} \int \Theta(k_{F_{B'}} - |\vec{k}|) \frac{M_{B'}^*}{E_{B'}^*(k)} d^3k, \quad (3)$$

where $E_B^*(k) = (k^2 + (M_B^*)^2)^{1/2}$, and where $J_i = \frac{1}{2} \forall i \in B$ is the spin of baryon i . In QMC, the scalar self-energy is modified to obtain Eq. (1), which requires care to be taken with the additional self-consistency.

Using these relations and fitting the couplings to saturation properties, the only independent quantities that still require definition are the proton and neutron Fermi momenta. These are constrained by requiring that the conserved total baryon density is equal to a selected value, and that the total electric charge of the system is zero. These conditions are given by

$$\rho_{\text{total}} = \sum_B \rho_B, \quad 0 = \sum_B Q_B \rho_B + \sum_\ell Q_\ell \rho_\ell. \quad (4)$$

3. INFINITE BARYONIC MATTER

Once the required self-consistent equations of the previous section have been satisfied, we can calculate the properties of dense matter. The species fractions Y_i of various particles at a wide range of densities can be calculated once all of the relevant Fermi momenta are determined, given that

$$Y_i = \rho_i / \rho, \quad \rho_i = \frac{(2J_i + 1)}{(2\pi)^3} \int \Theta(k_{F_i} - |\vec{k}|) d^3k = \frac{6k_{F_i}^3}{3\pi^2}. \quad (5)$$

The energy-density and pressure in QMC are analytically identical to those of QHD (as given in Ref. [3]), noting of course that now the effective mass has the quadratic form of Eq. (1).

We have assumed up to this point that at extremely high densities ($\rho > 3\rho_0$) hyperons will remain the correct degrees of freedom, however it is possible that at some density the concept of distinct baryons becomes inaccurate, and that the component quarks can become deconfined. In this case, we must consider the possibility of a phase transition to quark matter.

4. PHASE TRANSITIONS

The Gibbs conditions for a first-order phase transition between two phases (i, j) are that at the phase transition point, the following equilibria are achieved:

Thermal Equilibrium: The total temperature of each phase must be equal, thus $T_i = T_j$,

Mechanical Equilibrium: The total pressure of each phase must be equal, thus $P_i = P_j$,

Chemical Equilibrium: The independent chemical potentials of each phase must be equal, thus $\{\mu_\alpha\}_i = \{\mu_\alpha\}_j$.

It is possible that there exists a range of densities at which these conditions are met (and thus a mixed-phase exists), outside of which the phase with the greater pressure will be energetically favoured. Further details can be found in Refs. [4, 5]

We calculate the baryon phase EoS at $T = 0$ at increasing densities (using the independent chemical potentials as inputs to the quark-matter EoS) until we reach a point at which the pressure in each phase is equal (if it exists). This signals the onset of a mixed phase which we parameterize with the quark fraction $0 \leq \chi \leq 1$ up to the phase transition to pure quark-matter at $\chi = 1$. We then continue to calculate the quark-matter EoS with increasing density.

We use two quark-matter models; the MIT bag model [6] and the Nambu–Jona-Lasinio (NJL) model [7]. The former models constant current-quark masses, while the latter models the effect of dynamic chiral symmetry breaking, producing constituent-quark masses at low densities, and current-quark masses at large densities.

The species fractions for a hybrid EoS involving a hyperonic QMC baryon phase and an MIT bag model (using $B^{1/4} = 180$ MeV) quark phase are shown in Fig. 1 where we note the presence of baryon-, mixed-, and quark-phases.

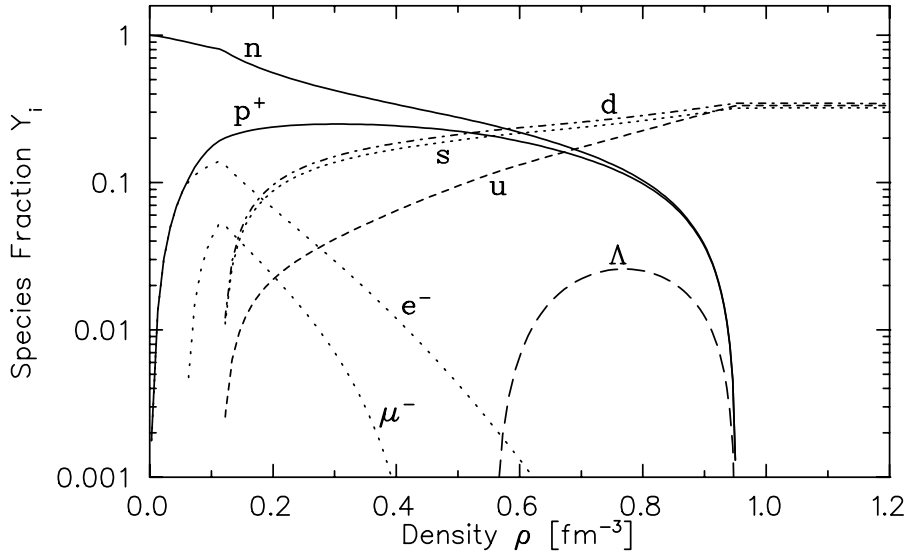


FIGURE 1. Species fractions Y_i for hyperonic QMC with a phase transition to a MIT bag model quark matter via a mixed phase. We note that with these parameters, the transition to a mixed phase occurs below saturation density, $\rho_0 = 0.16 \text{ fm}^{-3}$.

If we calculate the hybrid EoS using hyperonic QMC and NJL we find that the quark pressure remains lower than the baryon pressure for any density. This is a result of the large quark masses at low density and the relation between the pressure and Fermi momentum (via μ_q). As a consequence, we find that no phase transition from hyperonic QMC to NJL quark-matter is possible for any reasonable value of B . We do however find that the transition is possible from *nucleonic* QMC to NJL quark-matter, in which case the baryon phase is not significantly softened by the inclusion of hyperons.

5. STELLAR SOLUTIONS

In order to test these models against observations, we calculate properties of hybrid stars such as the total stellar mass and radius. The masses of these objects are comparatively easy to measure in the form of (particularly, binary) pulsars. The radius however has proven to be a greater challenge to measure.

In order to calculate the predicted properties of hybrid stars we use the EoS (which may include a mixed- or quark-phase) as input to the Tolman-Oppenheimer-Volkoff (TOV) equation

$$\frac{dP}{dR} = -\frac{G(P + \mathcal{E})(M(R) + 4\pi R^3 P)}{R(R - 2GM(R))}, \quad M(R) = \int_0^R 4\pi r^2 \mathcal{E} dr, \quad (6)$$

where \mathcal{E} and P are the energy density and pressure in the EoS, respectively.

The predicted values of mass and radius for QMC both with and without a phase transition to MIT bag model quark-matter are shown in Fig. 2. We note that the inclusion of a phase transition lowers the stellar mass for a star with a given central density, due to a further softening of the EoS.

6. CONCLUSIONS

The efficiency with which QMC allows one to model hyperon contributions highlights the importance of baryon structure. The lack of a phase transition between hyperonic QMC and NJL quark-matter indicates the importance of both hyperon degrees of freedom and dynamic chiral symmetry breaking, both of which must be treated with care. A transition is possible when one or both of these factors is neglected, but the physics must be *removed* by hand.

In order to achieve a Gibbs phase transition between a baryon phase and a quark-matter phase in which dynamical chiral symmetry breaking gives rise to constituent-quark masses, a moderately stiff baryon EoS is required, otherwise no such transition is possible. Such is the case for hyperonic QMC and NJL quark-matter.

While the QMC model at Hartree level successfully reproduces many properties of finite nuclei and stellar objects, the softness of the hyperonic/hybrid EoS (as evidenced by the maximum stellar mass) is unable to fully account for the most massive pulsars observed to date. We note that further improvements such as calculations at Hartree-Fock level (of particular interest are the Fock terms corresponding to the π meson) are currently in development.

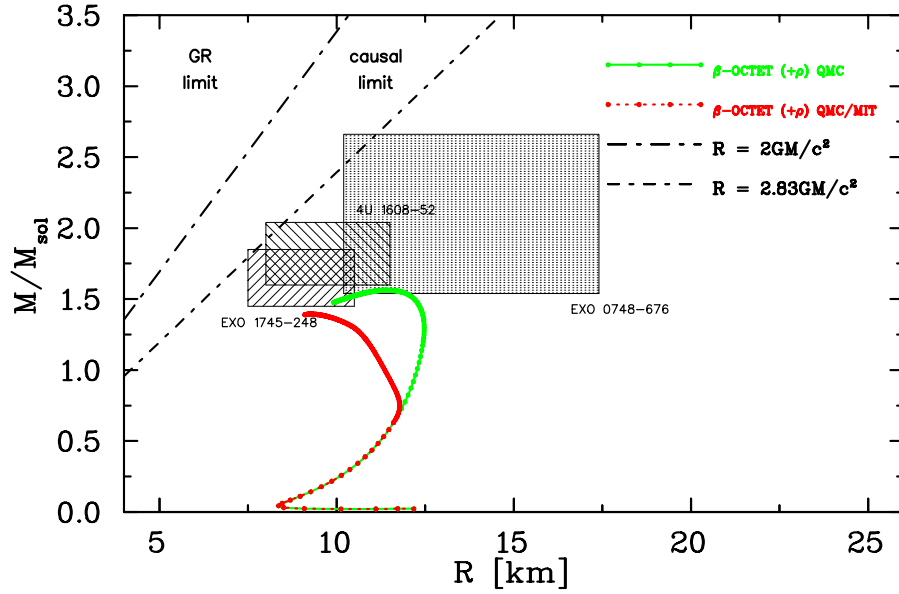


FIGURE 2. (Color online) Predicted total stellar mass and radius for hyperonic QMC with and without a phase transition to quark matter modelled with the MIT bag model. Also shown are the data points from Refs. [8] (EXO 0748-676), [9] (EXO 1745-248), and [10] (4U 1608-52).

ACKNOWLEDGMENTS

This research was supported by the Australian Research Council. The author would like to thank A. W. Thomas for his guidance and support, as well as D. B. Leinweber and A. G. Williams for their helpful discussions.

REFERENCES

1. J. Rikovska-Stone, P. A. M. Guichon, H. H. Matevosyan, A. W. Thomas. Nucl. Phys. A792:341-369, 2007 [doi:10.1016/j.nuclphysa.2007.05.011].
2. P. A. M. Guichon, A. W. Thomas, K. Tsushima. Nucl. Phys. A814:66-73, 2008 [doi:10.1016/j.nuclphysa.2008.10.001].
3. B. D. Serot, J. D. Walecka. Adv. Nucl. Phys.16:1-327, 1986.
4. J. D. Carroll, D. B. Leinweber, A. G. Williams, A. W. Thomas. Phys. Rev. C79:045810, 2009 [doi:10.1103/PhysRevC.79.045810].
5. J. D. Carroll. [arXiv:1001.4318 [hep-ph]].
6. A. Chodos, R. L. Jaffe, K. Johnson, C. B. Thorn, V. F. Weisskopf. Phys. Rev. D 9, 3471 (1974) [doi:10.1103/PhysRevD.9.3471].
7. Y. Nambu, G. Jona-Lasinio. Phys. Rev. 122, 345 (1961) [doi:10.1103/PhysRev.122.345].
8. F. Ozel. Nature 441, 1115 (2006) [doi:10.1038/nature04858].
9. T. Guver, F. Ozel, A. Cabrera-Lavers, P. Wroblewski. arXiv:0811.3979 [astro-ph].
10. F. Ozel, T. Guver, D. Psaltis. Astrophys. J. 693, 1775 (2009) [doi:10.1088/0004-637X/693/2/1775].